International Journal of Signal Processing, Image Processing and Pattern Recognition
Vol. 10, No. 9 (2017), pp.89-102
http//dx.doi.org/10.14257/ijsip.2017.10.9.09

Adaptive Method for the Analysis of Adhesive Particles Image

Wencheng Wang

College of Information and Control Engineering, Weifang University, Weifang 261061, China
wwcwfu@126.com

Abstract

An adaptive method for particle image is proposed to address the existing adhesion problem. In which the gray transformation and median filtering are applied for pre-processing on original image firstly. Then, the obtained image is segmented to a binary image with a threshold value. Next, distance transformation and watershed segmentation are performed on the morphologically processed binary image, and the watershed ridge line in the image is obtained. The boundary in adhesion is extracted by calculating the intersection between the original image and the segmented target area. Finally, the parameters of a particle such as area, perimeter, and particle diameter are calculated and the particle image analysis result is outputted. The experimental results show that this method is simple, convenient, and is suitable for the application in many industrial fields.

Keywords*: Adhesive Particles, Mathematical Morphology, Overlapping Particles, Watershed Segmentation*

1. Introduction

The geometric shape is one of the important features to describe the quality of a particle, and hence, parameter measurement is usually taken as an essential step during particle production. In recent years, with the development of electro-optical technology and image processing technique, the application of particle analysis technology based on machine vision is becoming increasingly popular, *e.g.*, the fully automatic cell analyser in medical fields, the nanoparticles analysis system in industrial applications, the seed selection system in agriculture, *etc.*. In general, the main steps in such systems are: the optical signal is converted into an electrical signal by using an image sensor and camera lens; an image capture card is used to convert the analog signal into a digital signal and send it to the processor; after pre-processing steps such as noise filtering and morphological operation, the image is segmented in order to obtain the edge of an object; finally, the mechanical equipment is controlled to work after calculating parameters such as perimeter and area of the individual objects[1-4].

However, the accuracy and practicability of traditional methods are generally based on well pre-processing of the particle image [5]. In practice, the particle objects in a captured image usually contact and adhere to each other; sometimes, the overlapping also occurs owing to the complex distribution of particles. Such a multi-particle cluster can seriously impact the subsequent statistical analysis, which may lead to major challenges in the final decision of the control equipment. In order to address this problem, an adaptive method is presented by combining distance transformation with the watershed algorithm based on particle parameter measurement [6-8]. Further, a particle granularity measuring system based on particle images is developed. This system completes feature extraction by using an image processing algorithm and executes automatic analysis by separating particles from complex backgrounds. The experiments demonstrate that the proposed method can separate the adhesive particle image in an effective and fast way. Further, it can provide a

ISSN: 2005-4254 IJSIP

quantitative description of the particle morphology, and is an effective method for fast quality analysis of granular objects. The proposed method generates satisfied results in production applications.

The remainder of this paper is organized as follows: In Section 2, the overall design of the proposed system is introduced. The image capture and pre-processing methods are described in Section 3. In Section 4, the key technique of segmenting adhesive particles is analyzed. The relevant experimental results and analysis are presented in Section 5. In Section 6, the conclusion and suggestions related to future work in this area are discussed.

2. Design of the System

The structure of the entire computer vision system used in the experiment is shown in Figure 1. The system consists of light source module that provides illumination for test samples, solid industrial camera and camera lens components used for obtaining an image, image capture card used for obtaining a digital image by performing analog-digital transformation, microprocessor system installed with image analysis software, high resolution color display used for displaying images, and output device[9-13].

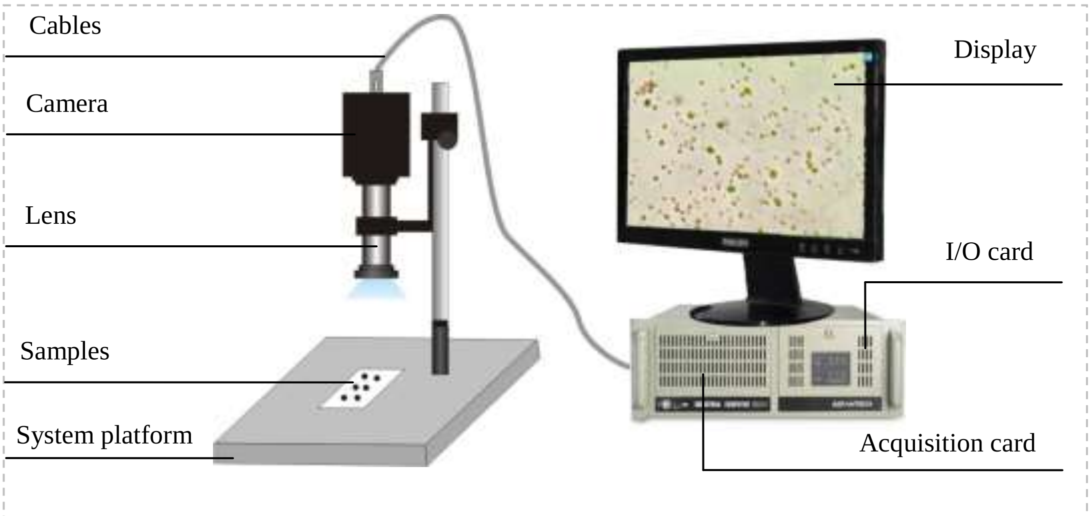

Figure 1. The Overall Structure of the System

The main components are described below:

- Industrial camera: A CMOS camera is suitable owing to the static nature of its collection of images and its low cost. The resolution of the camera is 2 million pixels.
- Camera lens: Based on the structure of the camera system holder, the system uses a camera lens that can fix the focus and has manual diaphragm regulation. The focal length of the lens is 16 mm.
- Light source: In the illumination module, the system uses an annular LED light source. This light source is installed below the camera, thus resulting in a high signal-to-noise ratio of the LED light source and more balanced illumination.
- Capture card: The capture card is installed in the expansion slot of the main board of the computer, thus allowing it to transfer the captured digital image to the computer for processing. The maximum capture speed is 10 fps.
- Output device: The computer is connected with an I/O interface card installed with relays in order to operate the outer electromechanical equipment.

Based on the actual conditions in which particles are tested and analyzed by the vision system, the system software includes four parts: image acquisition module, image preprocessing module, image segmentation module, and parameter analysis module. The image preprocessing module includes gray transformation and median filtering. The particle parameter analysis module is mainly used for completing particle measurement and for extracting important geometry information. Further, this module provides a histogram display of the area, perimeter, roundness, and elongation of a particle. The flowchart of the system is shown in Figure 2.

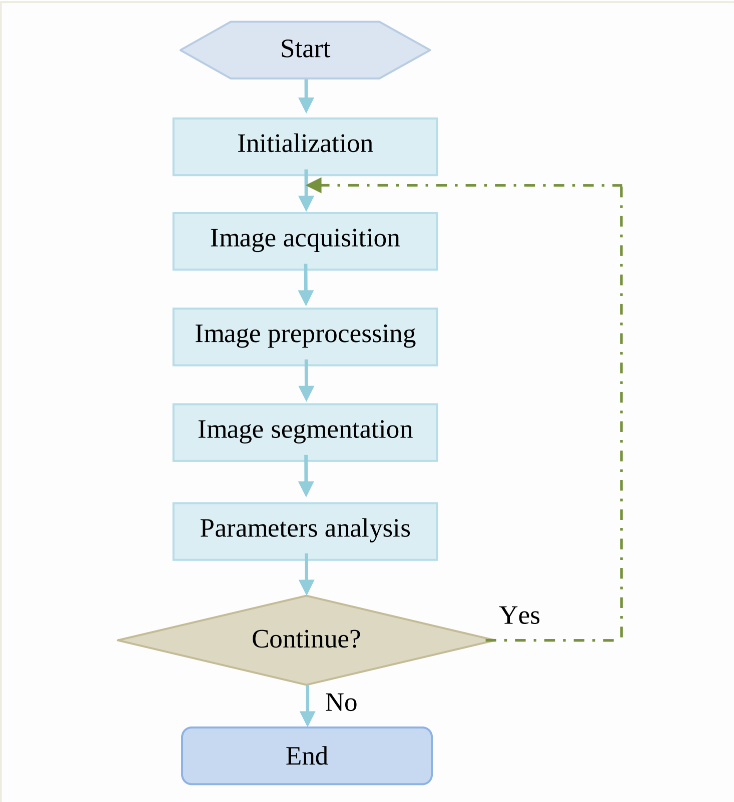

Figure 2. Process Flowchart of System

3. Pre-processing

3.1. Camera Calibration

The measuring system must be calibrated after configuring the camera and illuminating system well. The size of the measurement block used for calibration is the same, and hence, the size that each pixel actually represents can be determined only by obtaining the number of pixels per millimeter. The calibration procedure is as follows:

(i) Place the given dimensional calibration block on the working platform, capture an image, and then use the mouse to click on the pixel number x_1 on both sides of the obtained object.

(ii) Change the position of the calibration block continuously in the field of view in order to obtain 10 groups of data for object width, $x_1, x_2, \ldots, x_{10}$, and then determine the mean value $\bar{x}$.

(iii) Based on the given size L of the calibration blocks, the actual size represented by each pixel in the image can be determined for the current condition, and can be labeled as k mm/pixel. The computational formula is:

$$k = \frac{L}{\bar{x}} = \frac{L}{\sum_{i=1}^{10} x_i} \tag{1}$$

where k represents the actual size of a pixel. When the object is placed on the platform, the actual size of the object will be measured.

3.2. Gray Transformation

The image captured by the camera is a color image. Hence, gray transformation must be performed during digitization in order to improve the computation speed. The weighted average method is adopted and the sensitiveness principle of the human eye to color is taken into consideration. Thus,

$$\mathrm{Y} = \omega_R * R + \omega_G * G + \omega_B * B \tag{2}$$

where ω_R , ω_G , and ω_B are the corresponding weights of the R , G , and B color components, respectively, and Y is the pixel value of the corresponding points on the gray-scale map. The sensitiveness of the human eye to green is the highest, that to red is the second highest, and that to blue is the least, and hence, a relatively reasonable gray-level image can be obtained if $\omega_G > \omega_R > \omega_B$. The commonly used parameter setting is $\omega_R = 0.299$, $\omega_G = 0.587$, $\omega_B = 0.114$, for which the pixel value of the obtained gray level image is 256 levels.

3.3. Noise Reduction

In order to diminish the noise that results from image capturing, a median filter is adopted. The median filter is a nonlinear signal processing technology that can effectively suppress noise on the basis of the sorting statistical theory. The basic principle of the median filter is to use a sliding window with an odd number of points, and then use the median value of the gray level of each point in the window to replace the gray value of the central pixel in the window. The window W with an odd number of pixels is first determined, the pixels are ordered in the window based on the value of their gray levels, and then, the gray value at the center is used to replace the value of the central pixel in the window; this can be represented as:

$$g(x, y) = median\{ f(i-k, j-l), (k,l) \in W\} \tag{3}$$

where W is the selected template having an odd number of pixels. Figure 3 shows the frequently used median filter windows.

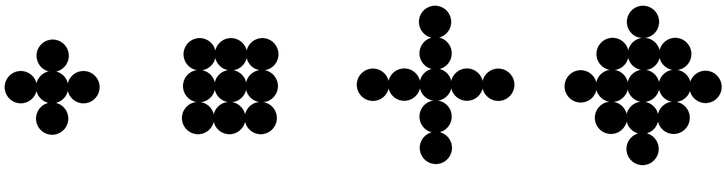

Figure 3. Commonly Used Median Filter Windows

The median filter method can address the image detail blurring phenomenon caused by linear filtering, reserve the edges of the image in an easy way, and filter the impulse interference and particle noise effectively. Hence, the median filter method is adopted to apply image intensification to a particle image. From Figure 4, it can be observed that the edge effect of the image after smoothing is intensified

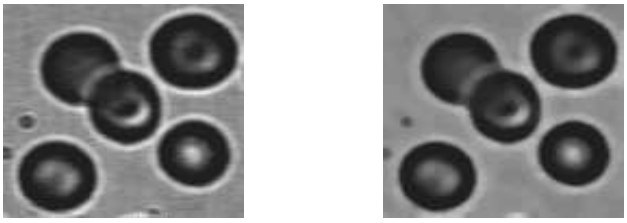

(a) Original Image (b) Filtered Image

Figure 4. Median Filtering

4. Image Segmentation

4.1. Binarization

Image segmentation is performed to distinguish the object from the background on the basis of certain specific features of the image. It is a labeling process with the important step of selecting a reasonable segmentation threshold. A pixel can be considered as belonging to the object if the gray value of that pixel exceeds the threshold value; otherwise, it is considered to belong to the background[1]. It is assumed that the original image is $f(x,y)$, the binary image is $g(x,y)$, and the threshold value is T, then:

$$g(x,y)=\begin{cases}1 & f(x,y)\geq T\\ 0 & f(x,y)<T\end{cases} \tag{4}$$

The image histogram obtained after the above process has obvious double peaks, and the gray levels of the foreground and background have approximately normal distribution; hence, it can be obtained by analyzing the trough of histogram. The threshold value is obtained by using an iterative method to analyze the histogram in order to make the system calculation have certain adaptability to environment. Iterative threshold method is based on progressive thought. In this method, the gray level is divided into two parts based on an initial threshold value. Then, the centers of these two parts are calculated separately, and the mean value of these centers is the new threshold value. This process is repeated iteratively until the former value and the latter value are smaller than a given error range and the algorithm converges. The calculation process is as follows:

Step 1: Compute the maximum gray value and minimum gray value of the image, label them as $P_{\max}$ and $P_{\min}$, respectively, and let the initial threshold value be $T_0=(P_{\max}+P_{\min})/2$;

Step 2: Segment the image into foreground and background based on the threshold value $T(k)\ (k=0,1,2,\ldots,k)$, and compute the average gray value of H_1 and H_2;

Step 3: Compute the new threshold value $T(k+1)=(H_1+H_2)/2$;

Step 4: If $T(K)=T(k+1)$, then, the obtained value is the threshold value; else, go to step 2 and perform iterative computations. The result after binarization is shown in Figure 5.

(a) Histogram (b) Binary image

Figure 5. Image Binarization

4.2. Morphological Processing

The image obtained after binarization has some holes and noise points in the particle image region. Hence, the holes must be filled and the noise points must be filtered. The seed filling algorithm and morphological opening algorithm can accomplish these objectives well.

In the seed filling method, the hypothesis is that at least one pixel point (called a seed) located inside the polygon area is known in advance. Then, using the algorithm, other pixels that are adjacent to the seed point and located inside the region are determined. If the adjacent points are not inside the region, then the edge of the region has been reached. If the adjacent points are inside the region, this point is considered as the new seed point, and a recursive search is performed. The search for the next pixel can occur in four directions during the search process.

The morphological opening algorithm consists of the process of erosion followed by dilation, which can be used for eliminating a small object by separating the particles at a slender point but not altering the area significantly. Erosion is the process of eliminating a boundary point and making the boundary shrink inward. It can be used for eliminating small and unwanted objects. The dilation of A by B, denoted as $A \oplus B$, is obtained by first reflecting B about its origin, and then, translating the result by x. All x such that A and reflected B translated by x have at least one point in common form the dilated set.

$$A \oplus B = \{x \mid (\hat{B})_x \cap A \neq \phi\} \tag{5}$$

where $\hat{B}$ denotes the reflection of B.

The erosion of A by B, denoted as $A \Theta B$, is the set of all x such that B translated by x is completely contained in A.

$$A \Theta B = \{x \mid (\hat{B})_x \subseteq A\} \tag{6}$$

The results of this processing are shown in Figure 6.

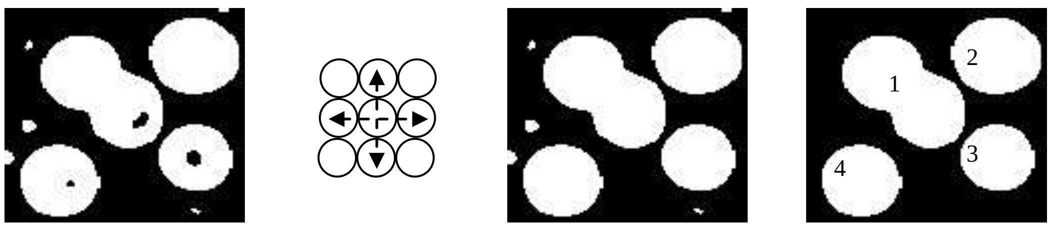

(a) Binary Image (b) 4-connection (c) After Filling (d) Opening Operation

Figure 6. Holes Filling and Morphological Processing

4.3. Separation of Adhesive Particles

The target particle can be extracted from the captured image by binarization to a gray image. However, owing to the location of the particles is random and the extracted particles may adhere to each other. It can be seen from Figure 6(d) that the actual number of particles inside the circle is five, while it is labeled as four in the image. Therefore, the next process of feature detection can be performed only after these adhesive particles are separated. The system uses a method based on distance transformation and watershed segmentation to completely extract the target.

(1) Distance transformation. Distance transformation is an operation on a binary image that converts the image into a gray-scale map. Assuming that the target to be segmented is white and the background is black in a binary image. Distance transformation will replace each white point, which represents the target in the binary image, with the shortest distance from this point to the background point. Such a transformation can make the target white zone correspond with one gray image whose margin gray value is small and inner gray value is large, thus enabling the gradient magnitude image to be used for watershed segmentation. Let us assume that an $M \times N$ binary image is denoted by a two-dimensional array $A_{M\times N} = [a_{ij}]$, where the pixel $a_{ij} = 1$ corresponds to a target point of the object and the pixel $a_{ij} = 0$ corresponds to a background point. Let $B = \{(x, y) \mid a_{ij} = 0\}$ be the background point set. Distance transformation performs the following computation for all the pixel points (i, j) in A:

$$d_{ij} = \min\{D_E[(i, j), (x, y)], (x, y) \in B\} \tag{7}$$

where the metric of $D_E[(i, j), (x, y)]$ uses the Euclidean distance, which can be specified in the form of equations as follows:

$$D_E[(i, j), (x, y)] = \sqrt{(i-x)^2 + (j-y)^2} \quad i = 1,2,2,\ldots,M,\ j = 1,2,3,\ldots,N \tag{8}$$

The binary image in Figure 7 (a) has two overlapping and connected circular regions, Figure 7(b) presents the distance transformation result of the image in Figure 7 (a), and Figure 7(c) corresponds to the three-dimensional display of the image in Figure 7 (b) after inversion. Thus, it is evident that the gradient image of the binary image becomes a gray image after distance transformation. Further, it possesses obvious topographic map characteristics, and thus, can be used for watershed segmentation.

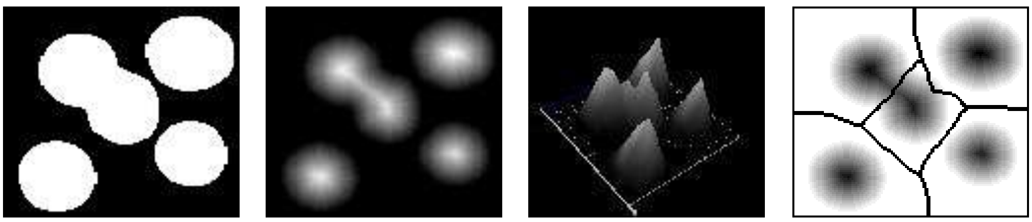

(a) Binary Image (b) Distance Transformation (c) 3D Map (d) Watershed Segmentation

Figure 7. Distance Transformation and Watershed Segmentation

(2) Watershed segmentation. The watershed algorithm was first introduced in the image segmentation field. In this algorithm, a gradient image is considered as a topographic map in geodesy. The gradient corresponds to the altitude, and areas with various gradient values in the image form a rugged landform model. In the model, the local minimum point of the gradient corresponds to the valley bottom, a point with a large gradient corresponds to a peak, the segmented region corresponds to the reception basin in a topographic map, and the edge of each reception basin, *i.e.*, a ridge, becomes a watershed. Thus, in a watershed, the points belonging to the same reception basin in the

original image are labeled as the same region, and image segmentation of the target is achieved, as shown in Figure 8.

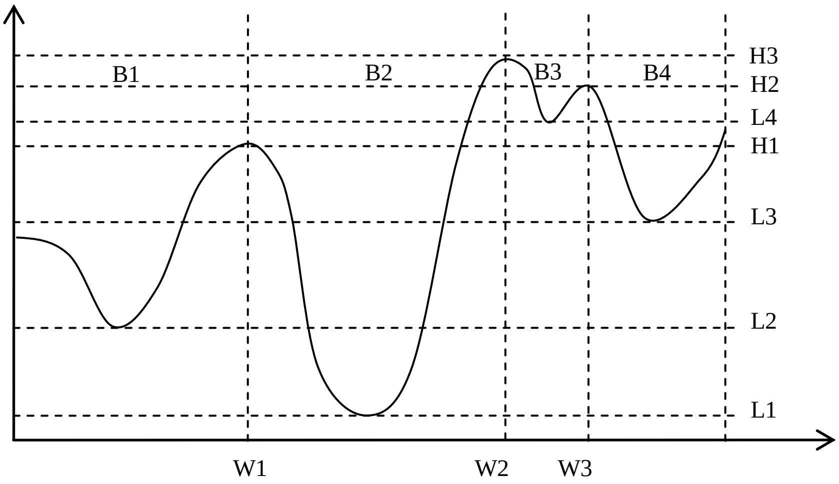

Figure 8. Diagram of the Watershed Algorithm

The soaking process of the watershed model consists of the following steps: A hole is opened at each local minimum point and the entire model is slowly immersed in water, soaking the basin with the overall minimum point first. The water level will rise gradually, cover the basin, and rise with the mountain slope. When it reaches the ridge, the water in the two adjacent basins will merge and the water will spill out. At this moment, a dam is established between the two basins to intercept the water until the entire model is immersed. This process divides the image into many valleys and basins, while the watershed is the dam used for separating these basins. From Figure 8, when the waterline reaches $L1$, water flows only into $B2$. When the waterline rises to $L2$, water also flows into the $B1$ basin. Water flows into $B4$ when the waterline rises to $L3$, whereas it flows into the $B3$ basin from the bottom of the valley when the waterline rises to $L4$. When the water level surpasses $H1$, the water in the $B1$ and $B2$ regions will meet and form dam $W2$. The watershed algorithm can provide a solution for weak margins, thus ensuring the continuity and closure of the edge of a segmented region. The image obtained after this process is shown in Figure 7(d).

The main advantage of the watershed segmentation method is that it can extract similar objects from the background and also obtain the margin of a segmentation area (*i.e.*, watershed) and the size of a segmentation area. The realization of such an algorithm mainly includes two processes: sorting and soaking.

4.4. Basic Parameters

(1) Area A is defined as the number of pixel points covered by a particle in a binary image, *i.e.*, the number of pixel points included in a zone boundary. Let us assume that the size of the image area $f(x,y)$ is $M \times N$, the pixel values in the binary image and object region are $f(x,y)=1$, and the pixel values of the background are $f(x,y)=0$. Then, the area of the particle is:

$$A=\sum_{x=0}^{M-1}\sum_{y=0}^{N-1} f(x,y) \tag{9}$$

(2) Perimeter P refers to the length of the contour line of the seed, and it is one of the indexes reflecting the particle size. Perimeter value refers to the distance of the boundary pixel of the object. For a straight line, it increases progressively by one pixel point for

consecutive pixels in the upward, downward, left, and right directions and the distance is 1. Further, there are four inclined directions including top left corner, bottom left corner, top right corner, and bottom right corner, and the distance between consecutive pixels in this inclined direction is $\sqrt{2}$ pixel. During perimeter measurement, the distance must be computed separately based on the connection type between pixels, which is shown in Figure 9.

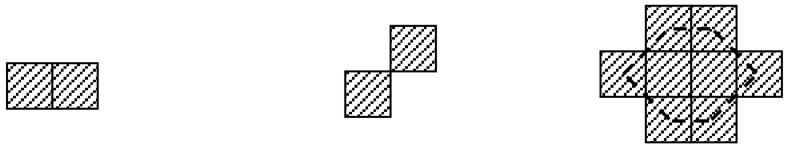

Figure 9. Example of Perimeter Calculation

(3) Roundness R is the degree to which the seed contour shape is round, and it is the characteristic parameter for computing the complexity of seed shape. The roundness calculation formula can be obtained from area and perimeter calculation:

$$R = \frac{4\pi \times A}{P^2} \tag{10}$$

For a circle with radius r, area is πr^2, and perimeter is $2\pi r$, the roundness is 1. A shape that is more round has a larger value of R; the maximum value of R is 1. For more complex shapes, the value of R is smaller and ranges between 0 and 1.

(4) Elongation E denotes the length-width ratio of rectangular particles, and it is used to describe the shape parameter of the particle. Let us assume that the length of the longer axis is L_1 and the length of the shorter axis is L_2. The expression for elongation is:

$$E = \frac{L_1}{L_2} \tag{11}$$

5. Parameter Analysis Experiment

We performed experiments to test the performance of the proposed algorithm. In these experiments, grains were selected to be used as particles. The particle diameter was approximately 2–5 mm, and the number of grain particles in the experiments were 55, 158, and 224. In order to intensify the contrast of the edge of a particle, each particle was placed on a black working platform. During the process, the perimeter (number of pixels) of the projected outline of each particle, area (number of pixels) of the region included by the outline, and the long axis (number of pixels) of the projected image of each particle can be obtained. Further, the actual perimeter and actual area of each particle can be calculated by using k, which represents the actual length of each pixel.

5.1. Experimental Image

As an example, 224 particles are used to demonstrate the process and effect of the experiment. Figure 10(a) is the original image. Figure 10(b) shows the result of threshold segmentation and it is a binary image. Figure 10(c) is the result obtained after applying the morphological opening algorithm; the slender noise point has been filtered. Figure 10(d) shows the distance transformation image based on Euclidean distance. Figure 10(e) is the watershed that can segment the adhesive grains into different zones. Figure 10(f) is the effect after watershed segmentation. Figure 10(g) is the contour map of the grain particles after segmentation. It can be observed that the segmentation result is effective.

Figure 10(h) shows the smallest rectangles of grain particles after segmentation. From Figure 10, it can be seen that the particles are separated from adhesive status successfully and the counting number is accurate.

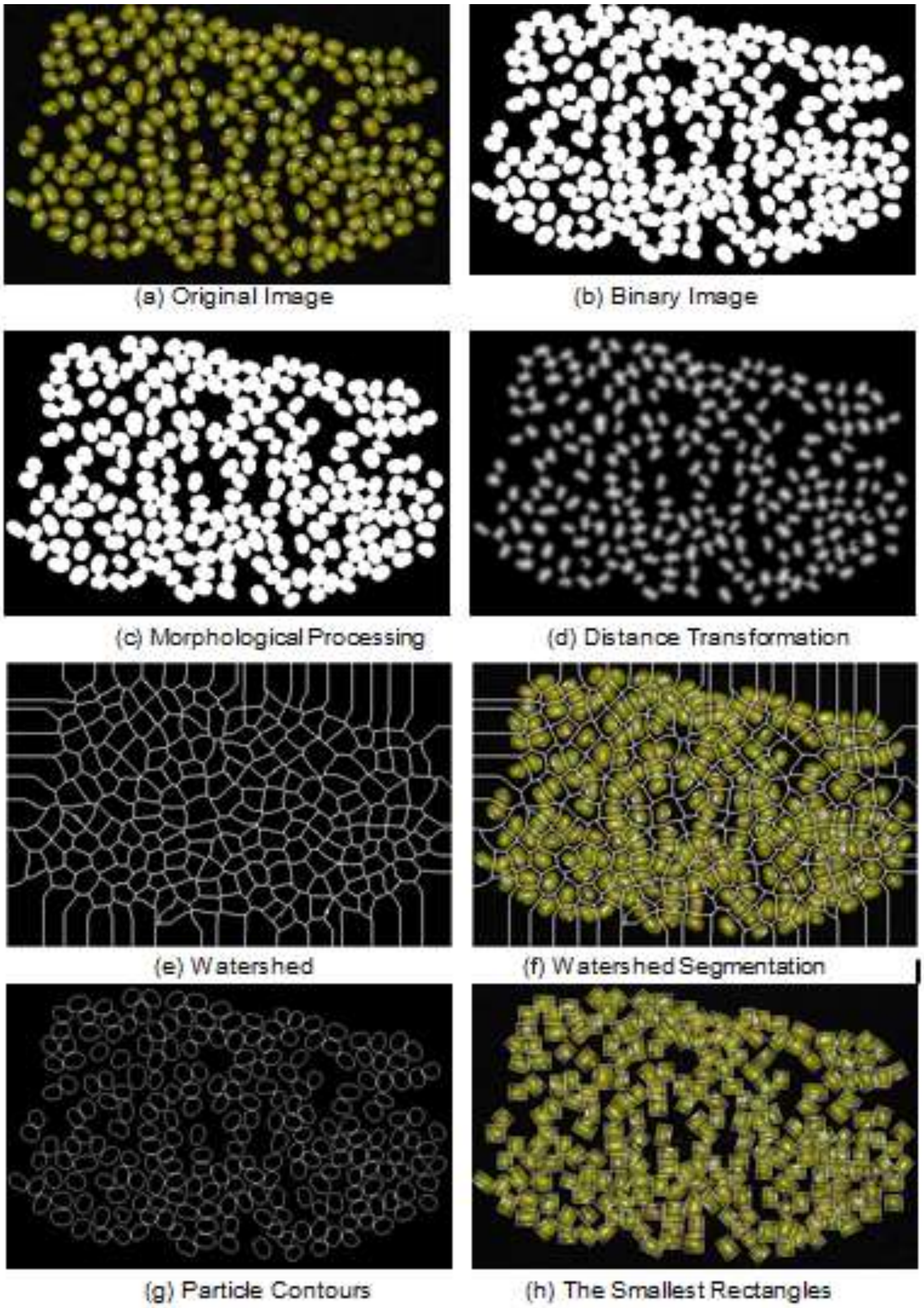

Figure 10. Experimental Results

5.2. Parameter Analysis

The parameter characteristics of a target grain can be easily obtained from the statistics on segmented image.

(1) Statistical analysis of grain area: The grain image obtained in the experiment by using the method described in Section 4.4 is analyzed, and then the area (the number of pixels) of each grain is computed according to the equation(9). The statistical data is shown in Figure 11.

From Figure 11, it can be seen that in the experimental images, the proportion of grain particles whose area is 400-700 pixels is large (more than 98%). The grain particles with an area of 550 pixels and 600 pixels cover most of the area, while those with an area of 400 pixels, 800 pixels, and 850 pixels cover only one, respectively.

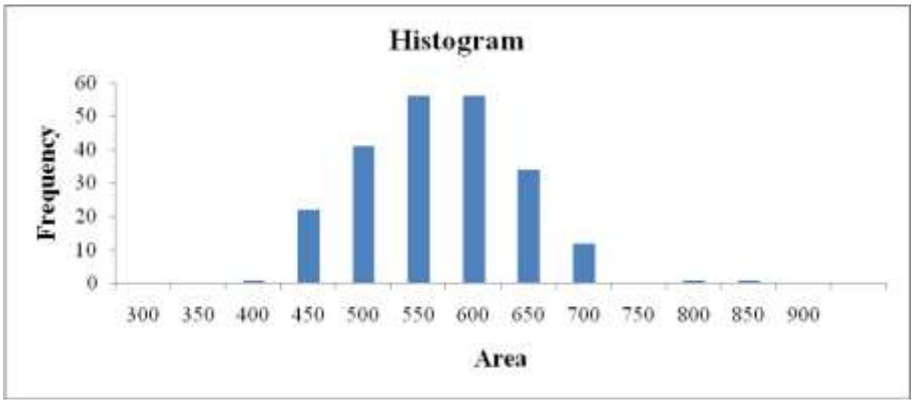

Figure 11. Area Histogram of Particles

(2) Statistical analysis of grain perimeter: The perimeter (the number of pixels) of each grain is determined according to the process described in Section 4.4, and the statistics are shown in Figure 12.

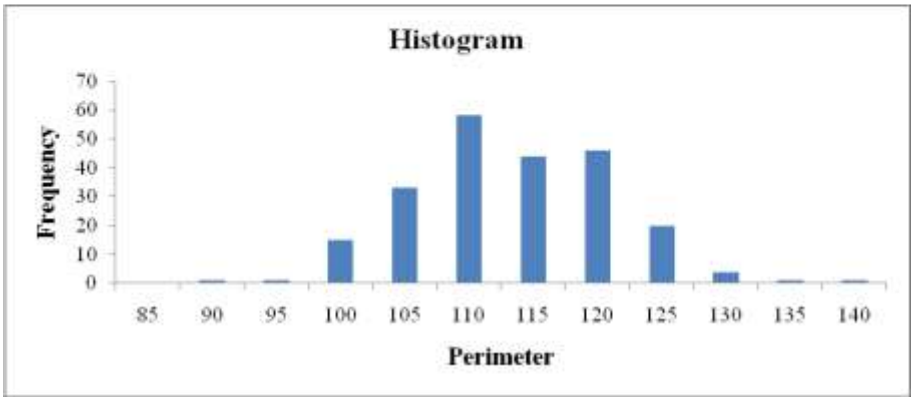

Figure 12. Perimeter Histogram of Particles

In Figure 12, it can be observed that the perimeter of grain particles is typically 100–125 pixels.

(3) Statistical analysis of grain roundness: The roundness of each grain is determined according to (10), and the statistical results are shown in Figure 13.

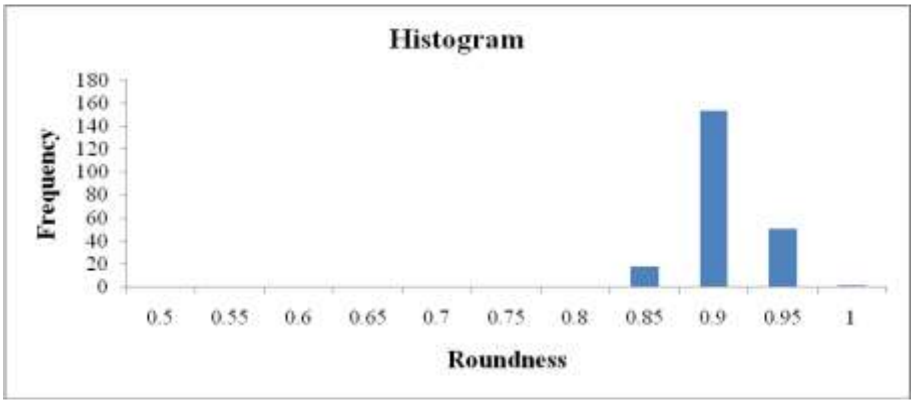

Figure 13. Roundness Histogram of Particles

From Figure 13, it can be observed that, in these experiments, the grain circularity is mainly 0.85–1. The proportion of roundness values exceeding 0.9 is more than 85%. Further, it has good fractal shape character.

(4) Statistical analysis of grain elongation: The length-width ratio of each grain is calculated according to Eq.(11), and the statistical results are shown in Figure 14.

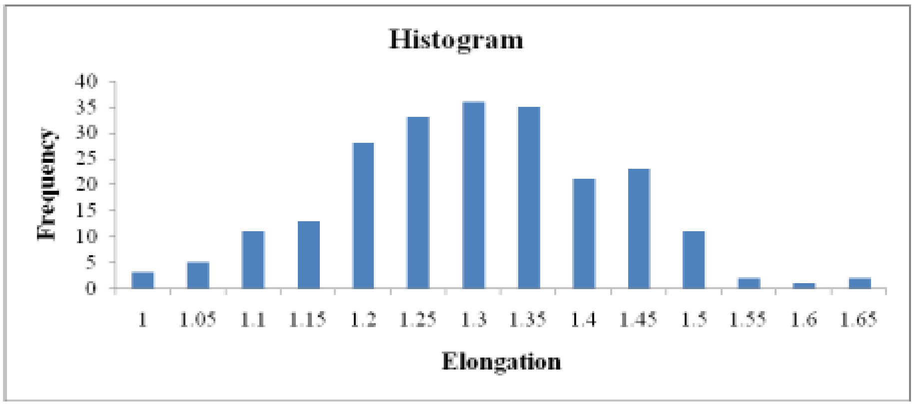

Figure 14. Elongation Histogram of Particles

From Figure 14, it can be observed that, in these experiments, the elongation values are mainly in the range 1–1.65, and the bounding shape is mainly rectangular.

6. Conclusions

An automatic system based on image processing technology is proposed for particle analysis in this paper. The working principle and key algorithms of the system are presented in details. The software mainly consists of four steps: image acquisition, image pre-processing, image segmentation and parameter analysis. Median filtering can weaken the noise interference in the original image; threshold segmentation can accomplish binarization; morphological processing can eliminate miscellaneous points; and watershed method based on distance transformation can complete the segmentation of adhesive particles. The experimental results show that this method is simple, fast, and effective. Further, the proposed method is successful in segmenting adhesive particles and it avoids the occurrence of insufficient-segmentation and over-segmentation. This algorithm can be applied to the fields of cell counting, biology, and industrial production.

Acknowledgments

This work has been supported by National Natural Science Foundation of China (Grant No. 61403283), Shandong Provincial Natural Science Foundation (No. ZR2013FQ036), the Spark Program of China(No. 2013XH06034), the Spark Program of Shandong Province(No. 2013XH06034) and Technology Development Plan of Weifang City(No. 201301015).

References

[1] F. Cloppet and A. Boucher, "Segmentation of complex nucleus configurations in biological images", Pattern Recognition Letters, vol. 31, no.8, **(2010)**, pp. 755-761.
[2] P. Karvelis, A. Likas and D. Fotiadis, "Identifying touching and overlapping chromosomes using the watershed transform and gradient paths", Pattern Recognition Letters, vol. 31, no. 16, **(2010)**, pp. 2474-2488.
[3] W. Wang, "A face detection method used for color images", International Journal of Signal Processing, Image Processing and Pattern Recognition, vol. 8, no. 2, **(2015)**, pp. 257-266.
[4] X. Long, W. Cleveland and Y. Yao, "Multiclass detection of cells in multi-contrast composite images", Computers in Biology and Medicine, vol. 40, no. 2, **(2010)**, pp.168-178.
[5] W. Wang and X. Cui, "An image-based system for measuring workpieces", Measurement & Control, vol. 47, no. 9, **(2014)**, pp.283–287.
[6] Y. Lu, "Study for automatic grain insect counting system based on image processing", Microcomputer Information, vol. 23, no. 8, **(2008)**, pp. 311-312, 2008.
[7] D. Mukherjee, Y. Potapovich, I. Levner and H. Zhang, "Ore image segmentation by learning image and shape features", Pattern Recognition Letters, vol. 30, no. 6, **(2009)**, pp. 615-622.
[8] R. A. Salinas, U. Raff and C. Farfan, "Automated estimation of rock fragment distributions using computer vision and its application in mining", IEEE Proceedings-Vision, Image, and Signal Processing, **(2005)**, pp.1-8.
[9] O. Schmitt, M. Hasse, "Morphological multi-scale decomposition of connected regions with emphasis on cell clusters", Computer Vision and Image Understanding, vol. 113, no. 2, **(2009)**, pp.188-201.
[10] N. Su and H. R. Xue, "The segmentation of overlapping milk somatic cells based on improved watershed algorithm", In: International Conference on Artificial Intelligence and Computational Intelligence, **(2009)**, pp.563-566.
[11] W. Wang, Y. Wang and T. Ji, "Grains automatic counting method based on computer vision", International Journal of Advancements in Computing Technology, vol. 4, no. 3, **(2012)**, pp. 345-351.
[12] H. Li and S. Li, "An Algorithm and Implementation for Image Segmentation", International Journal of Signal Processing, Image Processing and Pattern Recognition, vol. 9, no. 3, **(2016)**, pp. 125-132.
[13] Y. Zhou, L. B. Zeng and J. T. Liu, "A method for automatic colony counting based on image processing and its realization", Journal of Data Acquisition & Processing, vol. 18, no. 4, **(2003)**, pp. 460-464.

Author

Wencheng Wang, received the Ph.D. degree in 2011. And now he is working in Weifang University. His group has published and authored more than 40 papers on academic journals and conferences, four book chapters and 7 patents. His main research interests include digital information processing and intelligent computing.

